PLISKA
STUDIA MATHEMATICA

ПЛИСКА
МАТЕМАТИЧЕСКИ
СТУДИИ

Pliska Stud. Math. **29** (2018), 81–92

PLISKA
STUDIA MATHEMATICA

DYNAMIC FRACTURE OF A NANO-CRACK IN FINITE EXPONENTIALLY INHOMOGENEOUS PIEZOELECTRIC SOLID*

Marin Marinov, Tsviatko Rangelov, Petia Dineva

Aim of the study is to propose, develop, verify and apply in intensive simulations an efficient non-hypersingular traction boundary integral equation method (BIEM) for solution of anti-plane dynamic problem of a finite exponentially inhomogeneous piezoelectric solid with a nano-crack. The modelling approach is in the frame of continuum mechanics, wave propagation theory, the Gurtin and Murdoch surface elasticity theory and linear fracture mechanics. The simulations reveal the dependence of the stress concentration field on the electromechanical coupling, on the type and characteristics of the dynamic load, on the position-dependent material parameters, on the surface elasticity, on the size effect and on the wave-nanocrack-material gradient interaction.

1. Introduction

In a wide range of fields as structurel engineering, physics of solids, material science, biomechanics, non-destructive testing, geophysics, etc., a catastrophic fracture, failure and damage remains a major challenge. The fracture is gener-

2010 *Mathematics Subject Classification:* 35Q74, 74S15, 74H35.

Key words: Piezoelectricity, Exponential inhomogeneity, Surface elasticity, Anti-plane nanocrack, Time-harmonic load, SCF, BIEM.

*The authors acknowledge the support of the Bulgarian National Science Fund under the Grant No. DFNI-I 02/12.

ally initiates locally from a crack-tip, which leads to a global failure of materials through crack propagation across the entire structure. Fracture mechanics established on the basis of continuum mechanics provides a theoretical framework to describe the critical conditions at which a crack becomes mechanically unstable and starts to propagate. Understanding the nano-scale fracture behavior is critical for tailoring the mechanical properties of materials. It is known that classical continuum theory fails in predicting the material behavior at nano-scale where surface elasticity effects play an important role. A mechanical model taking into consideration the presence of surface stresses along the interface boundaries within the framework of the continuum mechanics was first proposed by Gurtin and Murdoch [1]. In this model the surface is assumed to be very thin, with different material properties in respect to the surrounding bulk material and it adheres to the bulk solid without slipping. As a consequence, the equilibrium equations along the surface of the interface yield to non-classical boundary conditions.

Anti-plane dynamic problems for elastic isotropic solids with nano-cracks are not available, but there exist limited number of papers for wave scattering by nano-holes and nano-inclusions, see Fang et al. [2, 3], Shodja and Pahlevania [4], Yang et al. [5], Zhang et al. [6]. Most of them apply the wave-function expansion method coupled with the surface elasticity theory.

Few results are known for piezoelectric materials with nano-holes, nano-inclusions and nano-cracks under anti-plane mechanical and in-plane electrical loads, see Xiao et al. [7], Fang et al. [8]. The problem of piezoelectric plane with a nano elliptic hole/crack subjected to far-field anti-plane mechanical and in-plane electric load is investigated by conformal mapping technique and complex variable approach in Xiao et al. [7]. The influences of the elliptic cavity shape ratio on the stress and electric displacement concentration factors are discussed. SH wave scattering by two piezoelectric nano-fibers in piezoelectric matrix is studied in Fang et al. [9] by the wave function expansion method, where the influence of the dynamic interactions between nano-inclusions on the electro-elastic wave fields is discussed.

New classes of advanced functionally graded piezoelectric materials (FGPM) are investigated intensively in our days due to their applications in smart intelligent systems. The authors results and a detail review of the existing in the literature solutions for dynamic behavior of 2D functionally graded piezoelectric infinite and finite solids with macro-cracks and/or macro-holes subjected to time-harmonic plane waves can be found in Dineva et al. [10]. The computational tool is a nonhypersingular traction BIEM based on fundamental solutions derived in a closed form by Radon transform for a restricted class of inhomogeneous materials.

Based on the above state-of-theart can be concluded that there are few results for homogeneous isotropic / anisotropic elastic / piezoelectric nano-cracked solids under dynamic loads and there are no any results for nano-cracks in continuously inhomogeneous elastic / piezoelectric isotropic / anisotropic materials.

The aim of this study is to consider the dynamic fracture behavior of a finite exponentially inhomogeneous piezoelectric transversely isotropic solid with a nano-crack subjected to time-harmonic anti-plane mechanical and in-plane electrical loads by BIEM taking into account the generalized surface elasticity effect in the frame of Gurtin and Murdoch model. At macro-scale the crack is finite line crack (Fig. 1 a), while at nano-scale a blunt crack (Fig. 1 b) with crack root presenting by a semi-circular shape of radius d is considered.

The paper is organized as follows: the statement of the problem is defined in Sect. 2., while its reformulation by integral equations along existing boundaries is given in Sect. 3., a series of numerical results is presented in Sect. 4., followed by conclusions in Sect. 5.

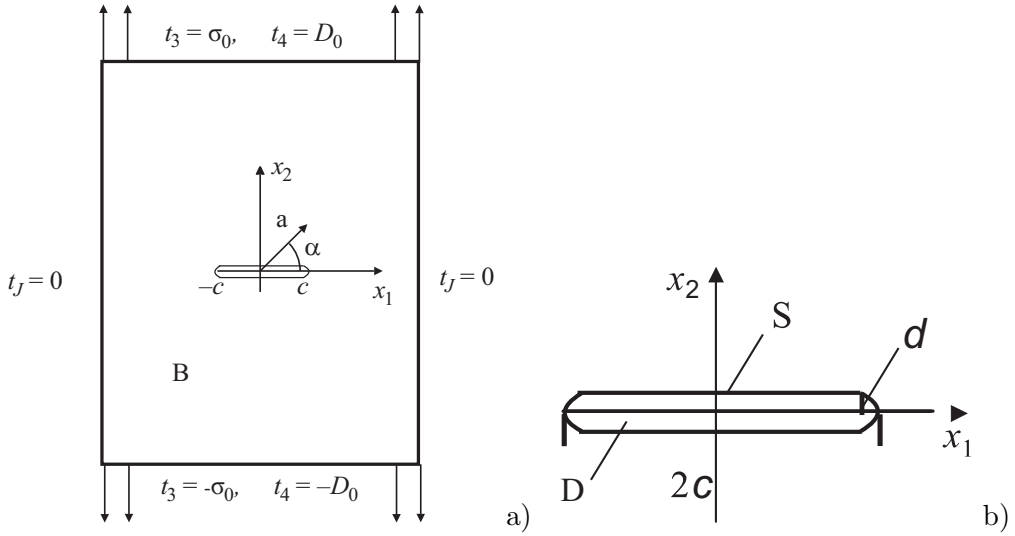

Figure 1: a) A rectangular exponentially inhomogeneous along direction α finite solid with a blunt nano-crack under time-harmonic uni-axial uniform mechanical traction t_3 and electrical displacement t_4 ; (b) Geometry of the blunt nano-crack

2. Problem statement

Consider a finite exponentially inhomogeneous along direction α transversally isotropic piezoelectric rectangular solid B with boundary ∂B in a Cartesian coordinate system $Ox_1x_2x_3$. The solid contains an internal nano-crack (Fig. 1 a). The model of the nano-crack is presented by a blunt crack G with boundary S and a crack root presenting by a semi-circular shape of radius d and the perimeter of the crack is $|S| = 2[2(c-d) + \pi d]$, with $d \ll c$, see Fig. 1 b. Assume that piezoelectric material shows hexagonal symmetry with respect to the axis Ox_2 and the poling axis is collinear with the Ox_2 axis. Consider anti-plane strain state with time-harmonic uni-axial along Ox_2 uniform mechanical traction $\bar{t}_3 = t_3 e^{i\omega t}$ and electrical displacement $\bar{t}_4 = t_4 e^{i\omega t}$, where ω is the frequency, and t_3, t_4 are the corresponding amplitudes. Since all field variables are time-harmonic, the common multiplier $e^{i\omega t}$ is suppressed in the following.

The only non-zero field quantities in plane $x_3 = 0$ are mechanical displacement $u_3(x,\omega)$, electrical displacement components $D_i(x,\omega)$, mechanical stress components $\sigma_{i3}(x,\omega)$, strain components $s_{i3}(x,\omega)$, electric field components $E_i(x,\omega)$ and electric potential $\phi(x,\omega)$, where the position vector is $x = (x_1, x_2)$ and $i = 1, 2$. Quasi-static approximation of piezoelectricity is assumed.

2.1. Governing equations

Following Landau and Lifshitz [11] the constitutive equation for linear piezoelectric bulk material is as follows:

$$\begin{aligned} \sigma_{i3}(x,\omega) &= c_{44}(x) s_{i3}(x,\omega) - e_{15}(x) E_i(x,\omega), \\ D_i(x,\omega) &= e_{15}(x) s_{i3}(x,\omega) + \varepsilon_{11}(x) E_i(x,\omega), \end{aligned} \tag{1}$$

where subscript $i = 1, 2$, $c_{44}(x), e_{15}(x), \varepsilon_{11}(x)$ are the variable with respect to position vector: shear stiffness, piezoelectric and dielectric permittivity characteristics. They are defined, together with the density $\rho(x)$ of the domain, by the inhomogeneous function $h(x) = e^{2\langle a,x\rangle}$, as follows

$$c_{44}(x) = c^0_{44} h(x), \quad e_{15}(x) = e^0_{15} h(x), \quad \varepsilon_{11}(x) = \varepsilon^0_{11} h(x), \quad \rho(x) = \rho^0 h(x), \tag{2}$$

where $\langle \cdot, \cdot \rangle$ is the scalar product in R^2; $a = (a_1, a_2)$, $a_1 = |a| \cos\alpha$, $a_2 = |a| \sin\alpha$, α is the inhomogeneity direction, $|a| = \sqrt{a_1^2 + a_2^2}$ is the inhomogeneity magnitude and $c^0_{44}, e^0_{15}, \varepsilon^0_{11}, \rho^0$ are the reference material properties, i.e. material properties for homogeneous material. Note that in inhomogeneous exponentially solid wave propagation phenomena exists only if the frequency of the applied load ω is greater than the critical frequency $\omega_0 = \sqrt{a_0/\rho_0}|a|$, see Rangelov et al. [12].

The strain–displacement and electric field–potential relations are:

$$s_{i3}(x,\omega) = u_{3,i}(x,\omega), \quad E_i(x,\omega) = -\phi_{,i}(x,\omega). \tag{3}$$

The balance equation in the absence of a body force and an electric charge is as follows:

$$\begin{aligned} &(c_{44}(x)u_{3,i}(x,\omega))_{,i} + (e_{15}(x)\phi_{,i}(x,\omega))_{,i} + \rho(x)\omega^2 u_3(x,\omega) = 0, \\ &(e_{15}(x)u_{3,i}(x,\omega))_{,i} - (\varepsilon_{11}(x)\phi_{,i}(x,\omega))_{,i} = 0. \end{aligned} \tag{4}$$

In Eqs. (3) and (4) summation convention over repeated indices is applied.

The constitutive equations (1) take the form presented in Eq. (5) if the following generalized notations are introduced: $u_J = (u_3, \Phi)$, $J = 3, 4$.

$$\sigma_{iJ} = C_{iJKl}u_{K,l}, \quad i,l = 1,2, \quad J,K = 3,4, \tag{5}$$

where $C_{iJKl} = C^0_{iJKl}h(x)$ and $C^0_{i33l} = \begin{cases} c^0_{44}, i = l \\ 0, \quad i \neq l \end{cases}$, $C^0_{i34l} = C^0_{i43l} \begin{cases} e^0_{15}, & i = l \\ 0, & i \neq l \end{cases}$, $C^0_{i44l} = \begin{cases} -\varepsilon^0_{11}, & i = l \\ 0, & i \neq l \end{cases}$ and Eq. (4) is reduced to

$$L(u) \equiv \sigma_{iJ,i} + \rho_{JK}\omega^2 u_K = 0, \tag{6}$$

here $\rho_{JK} = \begin{cases} \rho, & J = K = 3 \\ 0, & J = 4 \text{ or } K = 4 \end{cases}$.

2.2. Boundary conditions

2.2.1. Along the external solids boundary ∂B

Boundary conditions along the external boundary ∂B of the solid under consideration are prescribed traction $\bar{t}_J$:

$$t_J = \bar{t}_J, \quad \text{on } \partial B \tag{7}$$

where $t_J = \sigma_{iJ}n_i$ and $n = (n_1, n_2)$ is the outer normal vector to ∂B.

2.2.2. Along the blunt nano-crack's boundary S

In the frame of Gurtin and Murdoch [1] surface elasticity model the interface S between the blunt nano-crack and the finite exponentially inhomogeneous piezoelectric matrix M is an infinitely thin elastic isotropic layer which is coherent i.e. no slip, twist or wrinkling. In this case the surface mechanical strain ϵ^S_{l3}

in tangential direction l with respect to the interface boundary S is equal to the associated tangential strain in the abutting bulk piezoelectric matrix ϵ_{l3}^{M}, i.e. $\epsilon_{l3}^{S} = \epsilon_{l3}^{M} = \epsilon_{l3}$ and $u_3^S = u_3^M = u_3$. The constitutive equation for the bulk material is Eq. (1). The infinitely thin interface layer S is elastic isotropic with own surface elastic constant. The local constitutive equation for the elastic isotropic surface boundary S is as follows, see Luo and Wang [13], Xu and Dong [14]:

$$\sigma_{l3}^{S} = 2\mu^{S}\epsilon_{l3}^{S}, \quad s_{l3}^{S} = \frac{\partial u_3^S}{2\partial l}, \tag{8}$$

where the surface elastic stiffness constant μ^S is considered as known.

The crack is assumed to be electrically impermeable and in this case the electric field inside the crack is ignored and it may be thought as a low-capacitance medium with a potential jump $\Delta\phi = \phi^{+} - \phi^{-}$. The boundary condition for the normal component of the electrical displacement in this case is $D_n^S = 0$. The infinitely thin interface layer S is coherent, perfect bonded and in this case is satisfied the condition $D_l^S = D_l^M$.

The non-classical boundary condition in the surface elasticity theory of Gurtin and Murdoch takes into consideration a jump in the stresses as one move from the bulk material (matrix M) to the nano-crack surface S due to the presence of surface stress σ_{l3}^{S} along S. It states the following relation

$$t_3(x,\omega) = \sigma_{n3(x,\omega)} = -\frac{\partial \sigma_{l3}^{S}(x,\omega)}{\partial l}, \quad x \in S. \tag{9}$$

Here $\dfrac{\partial \sigma_{l3}^{S}(x,\omega)}{\partial l}$ is tangential derivative of tangential components of the stress defined in (8). Note that in the case of zero surface material characteristic $\mu^S = 0$, the non-classical boundary conditions (8) transforms into classical one for traction free surface of the impermeable crack.

Finally, the boundary condition for traction along the interface boundary S has the following form after substituting Eq. (8) in Eq. (9):

$$t_3^{M}(x,\omega) = -\mu^{S}\frac{\partial^2 u_3(x,\omega)}{\partial l^2}, \quad x \in S. \tag{10}$$

2.3. Boundary value problem

Consider the following BVPs

$$\left| \begin{array}{l} L(u^1) = 0 \quad \text{in } B, \\ t_J^1 = \bar{t}_J \quad \text{on } \partial B, \end{array} \right. \tag{11}$$

$$
\left|\begin{array}{l} L(u^2)=0 \quad \text{in } B\backslash G, \\ t_J^2=-t_J^1+t_J^M \quad \text{on } S, \\ t_J^2=0 \quad \text{on } \partial B. \end{array}\right. \tag{12}
$$

Since the BVP, Eqs. (6), (7), (10) is linear its solution is a superposition of BVPs, presented via Eqs. (11) and (12), so $u_J = u_J^1 + u_J^2$. The field u_J^1 is obtained by the dynamic load on ∂B in the crack free domain B, while u_J^2 is produced by the load $t_J^2 = -t_J^1 + t_J^M$ on S and zero boundary conditions on ∂B.

3. Non–hypersingular BIEM

Following after Wang and Zhang [15], Dineva et al. [10] the system of BVPs, presented by Eqs. (11) and (12) is transformed into an equivalent system of integro–differential equations on $\partial B \cup S$.

$$
\begin{aligned}
&\frac{1}{2}t_J^1(x) = C_{iJKl}n_i(x)\int_{\partial B}[(\sigma^*_{\eta PK}(x,y)u^1_{P,\eta}(y) \\
&-\rho_{QP}\omega^2 u^*_{QK}(x,y)u_P^1(y))\delta_{\lambda l} - \sigma^*_{\lambda PK}(x,y)u^1_{P,l}(y)]n_\lambda(y)d\partial B \\
&-C_{iJKl}n_i(x)\int_{\partial B} u^*_{PK,l}(x,y)t_P^1(y)d\partial B, \quad x\in\partial B,
\end{aligned} \tag{13}
$$

$$
\begin{aligned}
&t_J^c(x) = C_{iJKl}n_i(x)\int_S[(\sigma^*_{\eta PK}(x,y)u^2_{P,\eta}(y) \\
&-\rho_{QP}\omega^2 u^*_{QK}(x,y)u_P^2(y))\delta_{\lambda l} - \sigma^*_{\lambda PK}(x,y)u^2_{P,l}(y)]n_\lambda(y)d\Gamma \\
&+C_{iJKl}n_i(x)\int_{\partial B}[(\sigma^*_{\eta PK}(x,y)u^2_{P,\eta}(y) - \rho_{QP}\omega^2 u^*_{QK}(x,y)u_P^2(y))\delta_{\lambda l} \\
&-\sigma^*_{\lambda PK}(x,y)u^2_{P,l}(y)]n_\lambda(y)dS, \quad x\in S\cup\partial B.
\end{aligned} \tag{14}
$$

Here $x=(x_1,x_2)$ and $y=(y_1,y_2)$ denote the position vector of the observation and source point, respectively, $t_J^c(x) = \left\{\begin{array}{ll} -t_J^1(x)+t_J^M(x), & x\in S \\ 0, & x\in\partial B \end{array}\right.$, u^*_{JK} is a fundamental solution of Eq. (6), $\sigma^*_{iJQ} = C_{iJKl}u^*_{KQ,l}$ is the corresponding stress. The analytical expressions for the fundamental solution u^*_{JK} and details for its derivation can be found in Rangelov et al. [12].

Equations (13) and (14) constitute a system of integro–differential equations for the unknown u_J^2 and t_J^1 on the interface S and u_J^1, u_J^2 on the external boundary ∂B of the piezoelectric solid B.

4. Numerical solution and results

4.1. Numerical solution

The numerical procedure for the solution of the defined BVP follows the numerical algorithm developed and validated in Rangelov et al. [12], Dineva et al. [10].

The program code based on Mathematica 8 has been created. From numerical solution of Eqs. (13) and (14) the generalized displacement u_J at every internal point of B can be determined by using the corresponding representation formulae, see Gross et al. [16], Dineva et al. [10]. The normalized stress concentration field (SCF) and Electrical Field Concentration Factor (EFCF) close to the blunt crack-tip at the point $(\pm x_1, 0)$ is evaluating using the formulae

$$F^*_{III}((x_1,0),\omega) = \frac{\sigma_{23}((x_1,0),\omega)}{\sigma\sqrt{\pi c}}\sqrt{2\pi(x_1 \mp c)}, \quad |x_1| > c,$$
$$F^*_{E}((x_1,0),\omega) = \frac{E_3((x_1,0),\omega)}{\sigma\sqrt{\pi c}}\sqrt{2\pi(x_1 \mp c)}, \quad |x_1| > c,$$

where $E_3((x_1,0),\omega) = \dfrac{\phi((x_1,0),\omega)c_{44} - t_3((x_1,0),\omega)e_{15}}{\varepsilon_{11}c_{44} + e_{15}^2}, \quad |x_1| > c..$

4.2. Numerical results

The reference material used in the numerical examples is PZT-4, whose data are: $c^0_{44} = 2.56\times10^{10}N/m^2$, $e^0_{15} = 12.7C/m^2$, $\varepsilon^0_{11} = 64.6\times10^{-10}C/Vm$ and $\rho^0 = 7.5\times 10^3 kg/m^3$. The rectangular domain B is with dimensions $2\times10^{-8}m\times4\times10^{-8}m$. The interface S of the blunt nano-crack has a length $|S| = 1.0214\times10^{-8}m$, since $d = 0.0375\times c$ and $c = 2.5\times10^{-9}$.

It is used dimensionless surface parameter defined as $s = \dfrac{\mu^S}{2c_{44}dd_s}$, the surface constant $\mu^S = 6.091N/m$ is taken from the literature, see [17] and [18]. In the numerical results we get $d_s = 10.5747; 52.8733; 264.366, 2000$ that correspods to $s = 0.12; 0.024; 0.0048; \approx 0$.

In order to verify the numerical solution, a test example for a blunt nano-crack in a homogeneous rectangular plane under uni-axial uniform time-harmonic electro-mechanical load is solved The obtained solution at $s = 0$ recovers the result in Rangelov et al. [12]. In the homogeneous case critical frequency $\omega_0 = 0$ and the normalized frequency $\Omega = c\omega\sqrt{\rho^0/a_0}$ is introduced.

A parametric study is presented for the case of mechanical load with $\sigma_0 = 4\times10^8N/m^2$, $D_0 = 10^{-5}C/m^2$, see Fig. 1a, for the case of inhomogeneity with magnitude $\beta = 2|a|c = 0.2$ and direction $\alpha = 0$. SCF's at the left and at the right nano-crack tip are shown in Fig. 2 and Fig. 3 for the normalized frequency Ω greater than the critical one, which for the given β is equal to 0.1.

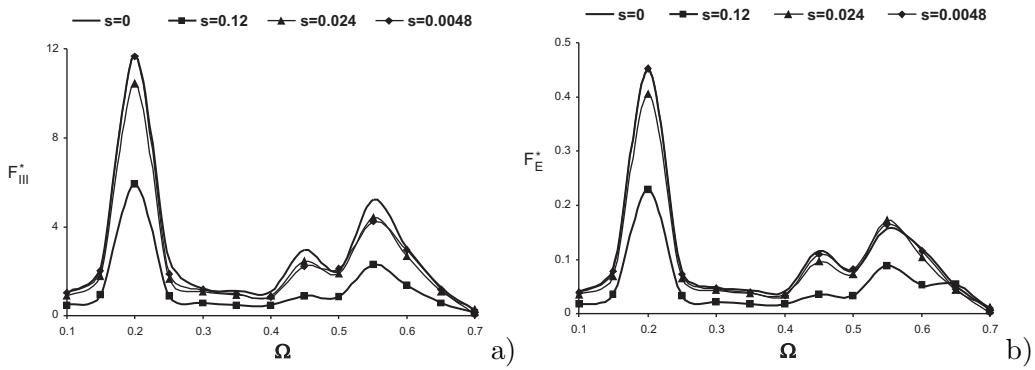

Figure 2: Normalized SCF and EFCF at the left nano-crack tip versus normalized frequency $\Omega \in (0.1, 0.7)$ at $\alpha = 0$, $\beta = 0.2$ for different values of s : a) F^*_{III}; b) F^*_E

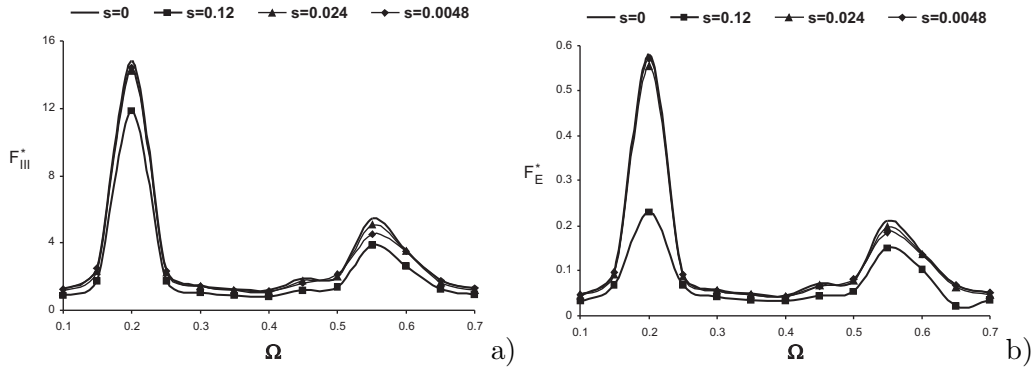

Figure 3: Normalized SCF and EFCF at the right nano-crack tip versus normalized frequency $\Omega \in (0.1, 0.7)$ at $\alpha = 0$, $\beta = 0.2$ for different values of s : a) F^*_{III}; b) F^*_E

The following conclusions can be made from the obtained results: (i) The SCFs for the inhomogeneity material is lower than for the homogeneous one but this effect is frequency dependent; (ii) For the inhomogeneity direction $\alpha = \pi/2$, the SCF is equal at points close to both left and right crack-tips; (iii) For the inhomogeneity direction $\alpha = 0$, the magnitude of the SCF at the left crack-tip and at the right crack-tip are different; (iv) For the frequencies above the critical ones the decreasing of the dimensionless surface parameter $s > 0$ provokes increasing of the SCF near the crack-tip in the whole considered frequency interval, while for frequencies below the critical ones the situation is reverse.

5. Conclusion

An anti-plane finite exponentially graded piezoelectric solid with a blunt nano-crack under time-harmonic electro-mechanical load is solved numerically by non-hypersingular traction BIEM which is developed and validated by Mathematica code. The BIEM computational tool is based on the fundamental solution derived in a closed form by Radon transform in conjunction with the surface elasticity model of Gurtin and Murdoch [1]. The simulations reveal that the dynamic non-uniform stress and the electric field distribution is a complex result of the mutual play of different key factors as: the type and the characteristics of the applied load; the type of material gradient and its magnitude and direction; the size of the blunt crack root curvature and surface elasticity effects.

REFERENCES

[1] M. E. Gurtin, A. I. Murdoch. A continuum theory of elastic material surfaces. *Arch. Ration. Mach. Anal.* **57** (1975), 291–323.

[2] X. Q. Fang, X. H. Wang, L. L. Zhang. Interface effect on the dynamic stress around an elliptical nano-inhomogeneity subjected to anti-plane shear waves. *Comput. Mater. Continua* **16**, *3* (2010), 229–246.

[3] X. Q. Fang, L. L. Zhang, J. X. Liu. Dynamic stress concentration around two interacting coated nanowires with surface/interface effect. *Meccanica* **48**, *2* (2013), 287–296.

[4] H. M. Shodja, L. Pahlevania. Surface/interface effect on the scattered fields of an anti-plane shear wave in an infinite medium by a concentric multi-coated nanofiber/nanotube. *Europ. J. Mech. A/Solids* **32** (2012), 21–31.

[5] Q. Yang, J. X. Liu, X. Q. Fang. Dynamic stress in a semi-infinite solid with a cylindrical nano-inhomogeneity considering nanoscale microstructure. *Acta Mech.* **223** (2012), 879–888.

[6] Q. F. Zhang, G. F. Wang, P. Schiavone. Diffraction of plane compressional waves by an array of nanosized cylindrical holes. *ASME, J. Appl. Mech.* **78** (2011), 021003.

[7] J. Xiao, Y. Hu, F. Zhang. A rigorous solution for the piezoelectric materials containing elliptic cavity or crack with surface effect. *ZAMM-Z. Angew.Math. Mech.* **96**, *5* (2016), 633–641.

[8] X. Q. Fang, Q. Yang, J. X. Liu, W. J. Feng. Surfaces/interface effect around a piezoelectric nano–particle in a polymer matrix under compressional waves. *Appl. Phys. Let.* **100** (2012), 151602.

[9] X. Q. Fang, J. X. Liu, L. H. Dou, M. Z. Chen. Dynamic strength araund two interacting piezoelectric nano–fibers with surfaces/interfaces in solid under electro–elastic wave. *Thin Solid Films* **520** (2012), 3587–3592.

[10] P. Dineva, D. Gross, R. Müller, T. Rangelov. *Dynamic Fracture of Piezoelectric Materials. Solutions of Time-harmonic problems via BIEM.* Solid Mechanics and its Applications, vol. **212**, Springer Int. Publ., Switzerland, 2014.

[11] D. L. Landau,E. M. Lifshitz. *Electrodynamics of Continuous Media.* Pergamon Press, Oxford, 1960.

[12] T. Rangelov, M. Marinov,P. Dineva. Time-harmonik behaviour of cracked piezoelectric solid by Boundary Integral Equation Method. *J. Theor. Appl. Mech.* **44**, *1* (2014), 51–68.

[13] J. Luo, X. Wang. On the anti–plane shear of an elliptic nano inhomogeneity. *Europ. J. Mech. A/ Solids* **28** (2009), 926–934.

[14] J. Y. Xu, C. Y. Dong. Surface and interface stress effects on the interaction of nano-inclusions and nano-cracks in an infinite domain under anti-plane shear. *Int. J. Mech. Sci.* **111–112** (2016), 12–23.

[15] C. Y. Wang, Ch. Zhang. 2D and 3D dynamic Green's functions and time-domain BIE formulations for piezoelectric solids. *Eng. Anal. Bound. Elem.* **29** (2005), 454–465.

[16] D. Gross, P. Dineva, T. Rangelov. BIEM solution of piezoelectric cracked finite solids under time-harmonic loading. *Eng. Anal. Bound. Elem.* **31**, *2* (2007), 152–162.

[17] P. Sharma, S. Ganti, N. Bhate. Effect of surfaces on the size–dependent elastic state of nanoinhomogeneities. *Appl. Phys. Lett.* **82** (2003), 535–537.

[18] H. L. Duan, J. Wang, Z. P. Huang, B. L. Karihaloo. Sizedependent effective elastic constants of solids containing nanoinhomogeneities with interface stress. *J. Mech. Phys. Solids* **53** (2005), 1574–1596.

Marin Marinov
Computer Science Department
New Bulgarian University
22, Montevideo Str.
1618 Sofia, Bulgaria
e-mail: mlmarinov@nbu.bg

Tsviatko Rangelov
Institute of Mathematics and Informatics
Bulgarian Academy of Sciences
Acad. G. Bonchev Str., Bl. 8
1113 Sofia, Bulgaria
*e-mail:*rangelov@math.bas.bg

Petia Dineva
Institute of Mechanics
Bulgarian Academy of Sciences
Acad. G. Bonchev Str., Bl. 4
1113 Sofia, Bulgaria
e-mail: petia@imbm.bas.bg